



**HAL**  
open science

# Techno-economic analysis of forward osmosis pre-concentration before an anaerobic membrane bioreactor: Impact of draw solute and membrane material

Sergi Vinardell, Gaetan Blandin, Federico Ferrari, Geoffroy Lesage, Joan Mata-Alvarez, Joan Dosta, Sergi Astals

## ► To cite this version:

Sergi Vinardell, Gaetan Blandin, Federico Ferrari, Geoffroy Lesage, Joan Mata-Alvarez, et al.. Techno-economic analysis of forward osmosis pre-concentration before an anaerobic membrane bioreactor: Impact of draw solute and membrane material. *Journal of Cleaner Production*, 2022, 356, pp.131776. 10.1016/j.jclepro.2022.131776 . hal-03709623

**HAL Id: hal-03709623**

**<https://hal.science/hal-03709623v1>**

Submitted on 21 Sep 2023

**HAL** is a multi-disciplinary open access archive for the deposit and dissemination of scientific research documents, whether they are published or not. The documents may come from teaching and research institutions in France or abroad, or from public or private research centers.

L'archive ouverte pluridisciplinaire **HAL**, est destinée au dépôt et à la diffusion de documents scientifiques de niveau recherche, publiés ou non, émanant des établissements d'enseignement et de recherche français ou étrangers, des laboratoires publics ou privés.

1 **Techno-economic analysis of forward osmosis pre-concentration before an**  
2 **anaerobic membrane bioreactor: Impact of draw solute and membrane material**

3

4 Sergi Vinardell<sup>a,\*</sup>, Gaetan Blandin<sup>b</sup>, Federico Ferrari<sup>c</sup>, Geoffroy Lesage<sup>d</sup>, Joan Mata-  
5 Alvarez<sup>a,e</sup>, Joan Dosta<sup>a,e</sup>, Sergi Astals<sup>a</sup>

6

7 <sup>a</sup> Department of Chemical Engineering and Analytical Chemistry, University of  
8 Barcelona, 08028, Barcelona, Spain

9 <sup>b</sup> Laboratory of Chemical and Environmental Engineering (LEQUiA), Institute of the  
10 Environment, University of Girona, 17003, Girona, Spain

11 <sup>c</sup> Eurecat, Centre Tecnològic de Catalunya, Water, Air and Soil Unit, 08242, Manresa,  
12 Spain

13 <sup>d</sup> Institut Européen des Membranes (IEM), Université de Montpellier, CNRS, ENSCM,  
14 34090, Montpellier, France

15 <sup>e</sup> Water Research Institute, University of Barcelona, 08028, Barcelona, Spain

16

17 \*Corresponding author (svinardell@ub.edu)

18

19

20 **Abstract**

21 This research investigated the impact of draw solute and membrane material on the  
22 economic balance of a forward osmosis (FO) system pre-concentrating municipal sewage  
23 prior to an anaerobic membrane bioreactor (AnMBR). Eight and three different draw  
24 solutes were evaluated for cellulose triacetate (CTA) and polyamide thin film composite  
25 (TFC) membranes, respectively. The material of the FO membrane was a key economic  
26 driver since the net cost of TFC membrane was substantially lower than the CTA  
27 membrane. The draw solute had a moderate impact on the economic balance. The most  
28 economically favourable draw solutes were sodium acetate and calcium chloride for the  
29 CTA membrane and magnesium chloride for the TFC membrane. The FO+AnMBR  
30 performance was modelled for both FO membrane materials and each draw solute  
31 considering three FO recoveries (50, 80 and 90%). The estimated COD removal  
32 efficiency of the AnMBR was similar regardless of the draw solute and FO membrane  
33 material. However, the COD and draw solute concentrations in the permeate and digestate  
34 increased as the FO recovery increased. These results highlight that FO membranes with  
35 high permselectivity are needed to improve the economic balance of mainstream AnMBR  
36 and to ensure the quality of the permeate and digestate.

37 **Keywords**

38 Forward osmosis (FO); Anaerobic membrane bioreactor (AnMBR); Anaerobic digestion;  
39 Reverse osmosis (RO); Draw solute; Techno-economic evaluation

## 40 **1. Introduction**

41 Climate change and resource depletion are pushing a paradigm shift in wastewater  
42 treatment plants (WWTPs) to maximise the recovery of resources and reduce the  
43 consumption of chemicals and energy (Zhang and Liu, 2022). In this new paradigm,  
44 membrane bioreactors play a central role since these technologies provide a physical  
45 barrier for solids and pathogens, which allows producing high-quality effluents and  
46 improving the performance of the bioreactor (Krzeminski et al., 2017).

47 Anaerobic membrane bioreactor (AnMBR), which combines membrane technology and  
48 anaerobic digestion, is an interesting biotechnology for municipal sewage treatment  
49 (Vinardell et al., 2020b). In AnMBRs, the sewage organic matter is transformed into  
50 methane-rich biogas and the biomass is completely retained by the membrane (Anjum et  
51 al., 2021; Hu et al., 2021). Several full-scale AnMBRs have already been implemented  
52 for the treatment of different types of industrial wastewater (Zhen et al., 2019). However,  
53 full-scale implementation of AnMBRs for municipal sewage treatment is limited because  
54 municipal sewage is typically less concentrated and represents a larger volumetric flow  
55 rate than industrial wastewater. The high volumetric flow rate and the low organic matter  
56 concentration of municipal sewage: (i) increases the AnMBR capital and operating costs,  
57 (ii) decreases the methane productivity per m<sup>3</sup> of sewage, and (iii) increases the total  
58 amount of methane dissolved in the effluent (Ferrari et al., 2019; Zahedi et al., 2021).  
59 Accordingly, it is important to develop technologies for sewage pre-concentration to  
60 improve the competitiveness of AnMBR for municipal sewage treatment.

61 Forward osmosis (FO) is an emerging membrane technology to pre-concentrate  
62 municipal sewage with low energy input, low fouling and high rejection of organic matter

63 (Awad et al., 2019; Wang and Liu, 2021). FO is spontaneously driven by the osmotic  
64 pressure difference between the feed solution and the saline draw solution (Blandin et al.,  
65 2021). The osmotic pressure gradient between both solutions drives the permeation of  
66 water from the feed solution to the draw solution through the dense FO membrane  
67 (Almoalimi and Liu, 2022). The most used materials for FO membranes are cellulose  
68 triacetate (CTA) and polyamide thin film composite (TFC) (Kim et al., 2022). The  
69 application of FO pre-concentration allows increasing the sewage organic matter  
70 concentration and decreasing the volumetric flow rate (Ansari et al., 2017). Moreover, a  
71 regeneration technology (e.g. reverse osmosis (RO), nanofiltration, membrane  
72 distillation) is typically used to re-concentrate the draw solution and produce high-quality  
73 water from the diluted draw solution (Cabrera-Castillo et al., 2021; Kim et al., 2017). The  
74 combination of FO, RO and AnMBR technologies for municipal sewage treatment can  
75 provide potential economic advantages in comparison with typical WWTP configurations  
76 (Vinardell et al., 2020a).

77 Draw solute selection is important since it affects the water and solute fluxes through FO  
78 membranes (Ansari et al., 2015; Arcanjo et al., 2020). Small inorganic solutes (e.g. NaCl,  
79 KCl) have been widely used as draw solutes because they feature high diffusivities and  
80 mitigate the detrimental effect of internal concentration polarisation (ICP) on water flux  
81 (Lutchmiah et al., 2014; Shaffer et al., 2015). However, these solutes generally feature  
82 high reverse solute fluxes (RSF) due to their high diffusivity (Zou et al., 2019). The RSF  
83 from the draw to the feed solution: (i) increases the salinity of the sewage and (ii)  
84 increases the draw solution replenishment costs (Ferby et al., 2020). The higher salinity  
85 in the pre-concentrated sewage could partially inhibit anaerobic bacteria with a direct  
86 impact on the AnMBR biogas production and effluent quality (both permeate and

87 digestate) (Vinardell et al., 2021). Therefore, the selection of the draw solute should  
88 contemplate both FO and AnMBR performance since solute selection can have a high  
89 impact on the technical and economic feasibility of combining both technologies.

90 Few studies have evaluated the impact of the draw solute on FO and anaerobic digestion  
91 performance (Ansari et al., 2015; Bacaksiz et al., 2021). Bacaksiz et al. (2021) evaluated  
92 the performance of different inorganic and organic draw solutes in the FO system and the  
93 inhibitory impact of these solutes on anaerobic digestion. The authors showed that the  
94 draw solute has a direct impact on the water flux and RSF of the CTA-FO membrane.  
95 Anaerobic digestion batch experiments showed that the RSF of inorganic draw solutes  
96 could inhibit the anaerobic digestion process, while organic draw solutes could increase  
97 methane production. Finally, Bacaksiz et al. (2021) conducted a preliminary economic  
98 analysis and reported that  $\text{CaCl}_2$ ,  $\text{MgCl}_2$ ,  $\text{HCOONa}$  and  $\text{CH}_3\text{COONa}$  were the most  
99 economically favourable draw solutes. However, the economic analysis only included the  
100 draw solute purchase cost, but did not include all the capital, operating costs and revenue  
101 (e.g. FO installation, labour, maintenance, membrane replacement, electricity production)  
102 influenced by the draw solute and FO membrane material. To the best of the authors'  
103 knowledge, the combined impact of draw solute and FO membrane material on the  
104 economic balance of a system combining FO and AnMBR technologies has not yet been  
105 evaluated. Accordingly, a detailed techno-economic analysis is needed to understand how  
106 these factors influence the economic feasibility of an FO+AnMBR system for municipal  
107 sewage treatment.

108 The main objective of this study is to evaluate the impact of draw solute and FO  
109 membrane material on the economic balance of an FO+AnMBR system for municipal  
110 sewage treatment. To this end, two FO membrane materials (CTA and TFC) and eight

111 different draw solutes (NaCl, MgCl<sub>2</sub>, KCl, CaCl<sub>2</sub>, Na<sub>2</sub>SO<sub>4</sub>, MgSO<sub>4</sub>, Ca(NO<sub>3</sub>)<sub>2</sub> and  
112 CH<sub>3</sub>COONa) were considered for the techno-economic analysis.

## 113 **2. Methodology**

### 114 **2.1 Design criteria and draw solutes selection**

115 Figure 1 shows the FO+AnMBR configuration evaluated in this study. The chosen  
116 configuration was a closed-loop scheme using a synthetic solution as a draw solution. The  
117 diluted draw solution was regenerated by means of RO to re-establish the initial osmotic  
118 pressure and to produce high-quality water. The draw solute was replenished (by topping  
119 up with salts) to keep the osmotic pressure constant in the loop despite losses of the draw  
120 solute through FO and RO membranes. The FO recovery was fixed at 80% because this  
121 is one of the most used FO recovery values in the literature for FO pre-concentration  
122 systems before anaerobic digestion (values range between 50 and 90%) (Ansari et al.,  
123 2018; Vinardell et al., 2021). The pre-concentrated municipal sewage was considered to  
124 be fed to an AnMBR configured as a continuous stirred tank reactor. The membranes  
125 were submerged in a separate membrane tank where gas sparging was applied to control  
126 the membrane fouling extent since this is the most common strategy for membrane  
127 fouling control in AnMBRs (Maaz et al., 2019). The AnMBR was considered to be  
128 operated at a solids retention time (SRT) of 60 days and at an hydraulic retention time  
129 (HRT) of 1 day (Vinardell et al., 2020a).

130 The selection of the draw solutes used for the economic evaluation was performed from  
131 available data for CTA and polyamide TFC commercial membranes. Regarding CTA  
132 membranes, seven inorganic and one organic draw solutes were evaluated: NaCl, MgCl<sub>2</sub>,  
133 KCl, CaCl<sub>2</sub>, Na<sub>2</sub>SO<sub>4</sub>, MgSO<sub>4</sub>, Ca(NO<sub>3</sub>)<sub>2</sub> and CH<sub>3</sub>COONa (Achilli et al., 2010; Ansari et

134 al., 2015). Regarding TFC membranes, three different inorganic draw solutes were  
135 evaluated: NaCl, MgCl<sub>2</sub> and MgSO<sub>4</sub> (Sanahuja-Embuena et al., 2019). This research did  
136 not include the same draw solutes for both membranes due to the limited data available  
137 in the literature regarding draw solute permeability in TFC membranes. The osmotic  
138 pressure of the draw solution before entering to the FO modules was considered to be 28  
139 bar for all the solutes, which is within the osmotic pressure range reported in previous  
140 studies (Achilli et al., 2010; Sanahuja-Embuena et al., 2019). The concentration of each  
141 draw solute at this osmotic pressure can be found in Table 1.

142 The economic analysis was conducted for a high-sized WWTP treating 100,000 m<sup>3</sup> d<sup>-1</sup> of  
143 municipal sewage (500,000 population equivalent). The municipal sewage was pre-  
144 filtered (~50 µm) before FO to prevent substantial fouling and clogging in the FO  
145 membranes and to decrease the amount of suspended solids fed to the AnMBR. The pre-  
146 filtered municipal sewage contained a total chemical oxygen demand (COD)  
147 concentration of 420 mg COD L<sup>-1</sup>, which was fractionated in biodegradable soluble COD  
148 (64.3%), inert soluble COD (19.1%), biodegradable particulate COD (7.1%) and inert  
149 particulate COD (9.5%) (Vinardell et al., 2020a).

## 150 **2.2 FO process design and modelling**

151 The water flux ( $J_w$ ) and RSF ( $J_s$ ) through dense FO membranes were modelled for all  
152 draw solutes and both membranes. Eq. (1) and Eq. (2) were used to model  $J_w$  and  $J_s$ ,  
153 respectively (Tirafferri et al., 2013). These equations considered that the active layer faced  
154 the feed side and included the effect of (i) dilutive ICP on the support layer, (ii)  
155 concentrative external concentration polarisation (ECP) on the active layer and (iii) RSF  
156 from the draw solution to the sewage (Blandin et al., 2015).

$$157 \quad J_w = A \cdot \left[ \frac{\pi_D \cdot e^{-J_w \frac{S}{D}} - \pi_F \cdot e^{\frac{J_w}{k}}}{1 - \frac{B}{J_w} \left( e^{-J_w \frac{S}{D}} - e^{\frac{J_w}{k}} \right)} \right] \quad \text{Eq. (1)}$$

$$158 \quad J_s = B \cdot \left[ \frac{c_D \cdot e^{-J_w \frac{S}{D}} - c_F \cdot e^{\frac{J_w}{k}}}{1 + \frac{B}{J_w} \left( e^{\frac{J_w}{k}} - e^{-J_w \frac{S}{D}} \right)} \right] \quad \text{Eq. (2)}$$

159 where  $J_w$  is the water flux ( $\text{L m}^{-2} \text{h}^{-1}$ ),  $J_s$  is the reverse draw solute flux ( $\text{g m}^{-2} \text{h}^{-1}$ ),  $A$  is  
 160 the water permeability ( $\text{L m}^{-2} \text{h}^{-1} \text{bar}^{-1}$ ),  $B$  is the draw solute permeability ( $\text{L m}^{-2} \text{h}^{-1}$ ),  $\pi_D$   
 161 is the osmotic pressure in the draw solution (bar),  $\pi_F$  is the osmotic pressure in the feed  
 162 solution (bar),  $c_D$  is the draw solute concentration in the draw solution ( $\text{g L}^{-1}$ ),  $c_F$  is the  
 163 draw solute concentration in the feed solution ( $\text{g L}^{-1}$ ),  $k$  is the mass transfer coefficient of  
 164 the draw solute ( $\text{L m}^{-2} \text{h}^{-1}$ ),  $D$  is the self-diffusion coefficient of the draw solute ( $\text{L m}^{-1} \text{h}^{-1}$ )  
 165 and  $S$  is the membrane structural parameter (m).  $A$ ,  $B$  and  $S$  parameters are widely used  
 166 in FO research because they allow comparison of FO performance regardless of the  
 167 operating conditions (Tiraferrri et al., 2013).

168 The intrinsic membrane parameters (i.e.  $A$  and  $S$ ) for CTA and TFC membranes were  
 169 obtained from Coday et al. (2013) and Sanahuja-Embuena et al. (2019), respectively. The  
 170 parameter  $B$ , which depends on both the membrane and the draw solute, was obtained  
 171 from Achilli et al. (2010) and Ansari et al. (2015) for CTA membrane, and from Sanahuja-  
 172 Embuena et al. (2019) for TFC membrane. In these publications, the CTA membrane was  
 173 a commercial FO membrane from Hydration Technology Innovations (HTI) (Albany,  
 174 USA) and the TFC membrane was a commercial FO membrane from Aquaporin  
 175 (Kongens Lyngby, Denmark) (Sanahuja-Embuena et al., 2019). HTI CTA membrane and  
 176 Aquaporin TFC membrane parameters  $A$ ,  $B$  and  $S$  were chosen as they were available in  
 177 the literature and are representative for commercial CTA and TFC membranes. Detailed

178 information about the A, B and S parameters as well as about the properties of the  
179 different draw solutes can be found in Table 1.

### 180 **2.3 Modelling AnMBR performance**

181 The AnMBR performance was modelled for the different FO alternatives (i.e. draw  
182 solutes, membrane materials and FO recoveries) to calculate the COD removal, the  
183 amount of methane recovered and the quality of the permeate. The presence of draw  
184 solute in the pre-concentrated sewage due to RSF could partially inhibit anaerobic  
185 biomass (i.e. Na<sup>+</sup>, K<sup>+</sup>, Ca<sup>2+</sup>, Mg<sup>2+</sup>), introduce an electron acceptor (i.e. SO<sub>4</sub><sup>2-</sup> and NO<sub>3</sub><sup>-</sup>)  
186 and/or introduce an electron donor (i.e. CH<sub>3</sub>COO<sup>-</sup>). The concentration of each draw solute  
187 in the AnMBR influent can be found in Table S1 of the supplementary information.

188 A steady state mass balance was used to model the AnMBR including a non-competitive  
189 inhibition function to determine the impact of draw solute concentration on anaerobic  
190 digestion performance (Eq. (3)). Subsequently, the total organic matter concentration in  
191 the AnMBR permeate was calculated using Eq. (4):

$$192 \quad Q_0 \cdot S_{S,0} - k_{m,ac} \cdot \frac{S_S}{S_S + K_{S,ac}} \cdot \frac{K_{I50}}{K_{I50} + S_{cat}} X_{ac} \cdot V = Q_e \cdot S_S \quad \text{Eq. (3)}$$

$$193 \quad S_e = S_S + S_I \quad \text{Eq. (4)}$$

194 where  $Q_0$  is the pre-concentrated sewage flow rate ( $\text{m}^3 \text{d}^{-1}$ ),  $S_{S,0}$  is the biodegradable  
195 organic matter (particulate and soluble) concentration in the pre-concentrated sewage ( $\text{kg}$   
196  $\text{COD m}^{-3}$ ),  $k_{m,ac}$  is the specific maximum uptake rate for acetogenic methanogens ( $\text{kg}$   
197  $\text{COD kg}^{-1} \text{COD}_{\text{cell}} \text{d}^{-1}$ ),  $S_S$  is the soluble biodegradable organic matter concentration in  
198 the AnMBR and in the permeate ( $\text{kg COD m}^{-3}$ ),  $K_{S,ac}$  is the half-saturation constant for  
199 acetogenic methanogens ( $\text{kg COD m}^{-3}$ ),  $K_{I50}$  is the 50% inhibitory constant for the draw

200 solute ( $\text{kg COD m}^{-3}$ ),  $S_{\text{cat}}$  is the cation concentration (i.e.  $\text{Na}^+$ ,  $\text{K}^+$ ,  $\text{Ca}^{2+}$ ,  $\text{Mg}^{2+}$ ) of the draw  
201 solute in the AnMBR ( $\text{kg COD m}^{-3}$ ),  $X_{\text{ac}}$  is the biomass concentration of acetogenic  
202 methanogens, which was considered to be a 10% of the biomass ( $\text{kg COD}_{\text{cell}} \text{m}^{-3}$ )  
203 (Ariesyady et al., 2007),  $V$  is the volume of the AnMBR ( $\text{m}^3$ ),  $Q_e$  is the permeate flow  
204 rate ( $\text{m}^3 \text{d}^{-1}$ ),  $S_e$  is the total soluble organic matter concentration in the AnMBR permeate  
205 ( $\text{kg COD m}^{-3}$ ) and  $S_I$  is the soluble inert organic matter concentration in the influent ( $\text{kg}$   
206  $\text{COD m}^{-3}$ ). The model parameters used in Eq. (3) can be found in Table S2† of the  
207 supplementary material. Eq. (3) and Eq. (4) assumed that: (i) methanogenesis is the rate-  
208 limiting step, (ii) all the biodegradable particulate organic matter is solubilised in the  
209 AnMBR because of the high SRT (60 days), (iii) particulate organic matter hydrolysis  
210 does not generate soluble inert material, (iv) the AnMBR waste sludge flow rate is  
211 negligible compared to the permeate flow rate and (v) the  $\text{KI}_{50}$  values are literature  
212 averages and potential acclimation to inhibitors was not considered.

213 The methane production was calculated considering: (i) the biodegradable COD removed  
214 in the AnMBR, (ii) the presence of electron acceptors (i.e.  $\text{SO}_4^{2-}$  and  $\text{NO}_3^-$ ) from the draw  
215 solution that could consume part of the COD, (iii) the presence of external COD coming  
216 from the draw solution (i.e. acetate) that could be an additional organic source for  
217 methane production and (iv) that a fraction on the methane remains dissolved in the  
218 effluent, which was calculated with Henry's law. It was considered that the organic matter  
219 consumed when sulphate and nitrate were contained in the pre-concentrated sewage  
220 corresponded to  $2.01 \text{ mg COD mg}^{-1} \text{SO}_4^{2-}\text{-S}$  and  $2.86 \text{ mg COD mg}^{-1} \text{NO}_3^-\text{-N}$ , respectively  
221 (Metcalf & Eddy, 2014).

## 222 **2.4 Costs and revenue calculation**

223 Draw solution has a direct impact on the FO capital and operating costs since it affects  
224 the water and the draw solute RSF through FO membranes. The RSF could also impact  
225 the amount of methane recovered in the AnMBR and the quality of the permeate. This  
226 section describes the costs and revenue considered for the economic evaluation. The cost  
227 calculation was conducted considering a fixed FO recovery of 80% and a draw solution  
228 osmotic pressure of 28 bar for all draw solutes and FO membrane materials (see Section  
229 2.1). It is worth mentioning that the costs and revenue that were not influenced by the  
230 draw solute or the FO membrane material were not considered for the economic  
231 evaluation (e.g. AnMBR capital and operating costs, RO capital costs, energy  
232 consumption, water production) since these costs and revenue are assumed to be similar  
233 regardless of the draw solute and FO membrane material used. Table S3 of the  
234 supplementary material shows detailed information about the parameters used for costs  
235 and revenue calculations.

#### 236 **2.4.1 FO capital and operating costs**

237 The methodology used to calculate the capital costs of the FO system can be found in  
238 Vinardell et al. (2020a), who adapted the methodology proposed by Blandin et al. (2015)  
239 to estimate the FO costs. Briefly, the capital costs of the FO system were estimated  
240 considering relationships with capital costs of typical full-scale spiral wound RO systems  
241 since (i) RO systems are rather similar to FO systems and (ii) there are more data available  
242 concerning the costs of RO systems than FO systems (Blandin et al., 2015). Firstly, a  
243 benchmark RO scenario was established, which corresponded to an RO installation  
244 requiring a similar membrane area than the FO installation using NaCl as a draw solute.  
245 The capital cost of the benchmark RO scenario was estimated (i) considering an RO  
246 membrane cost of 21 € m<sup>-2</sup> (Valladares Linares et al., 2016) and (ii) using the RO cost

247 distribution shown in Table S43 of the supplementary material. Second, the capital cost  
248 of the FO system for the NaCl was estimated (i) considering an FO membrane cost of 55  
249 £ m<sup>-2</sup> (49 € m<sup>-2</sup>) (Valladares Linares et al., 2016) and (ii) considering that specific cost  
250 contributors of the RO system could be partially (or totally) extendible to FO capital costs  
251 (e.g. civil engineering, equipment and materials, pumps) (Table S43). Finally, the FO  
252 capital costs for all the other draw solute scenarios were calculated from the FO capital  
253 costs of the NaCl scenario and considering that specific cost contributors were dependent  
254 on the FO membrane area (Table S43). The capital costs dependent on the FO membrane  
255 area were included in the economic evaluation since the costs that did not depend on the  
256 FO membrane area were not influenced by the draw solute and, therefore, are out of the  
257 scope of the present study.

258 The operating costs of the FO system accounted for membrane replacement, labour and  
259 maintenance. The membrane replacement cost was calculated assuming a membrane  
260 lifetime of 4 years (Yangali-Quintanilla et al., 2015). The labour and maintenance costs  
261 were considered to be dependent on the size of the FO installation. Specifically, the labour  
262 and maintenance costs accounted for 1% and 2.25% of the capital costs, respectively  
263 (Fritzmman et al., 2007; Vinardell et al., 2020a).

#### 264 **2.4.2 Draw solution replenishment costs**

265 The draw solution needs to be replenished due to losses of draw solute through both FO  
266 and RO membranes. Draw solute losses through FO membranes were calculated for each  
267 solute using Eq. (2) (see Section 2.2), while the draw solute losses through RO  
268 membranes were calculated using the Reverse Osmosis System Analysis (ROSA)  
269 software (Filmtec Corporation, US). Detailed information of the input parameters to

270 ROSA can be found in Table S5 of the supplementary material. The purchase cost of each  
271 draw solute was obtained from Bacaksiz et al. (2021) and is reported in Table 1.

### 272 **2.4.3 Energy production**

273 The energy production was calculated considering a methane calorific value of 55 MJ kg<sup>-1</sup>  
274 <sup>1</sup> (Metcalf & Eddy, 2014). The produced methane was combusted in a CHP unit with  
275 electrical and thermal efficiencies of 33 and 55%, respectively (Riley et al., 2020;  
276 Vinardell et al., 2021). The capital and operating costs of the CHP unit were 712 € kW<sub>el</sub><sup>-1</sup>  
277 <sup>1</sup> and 0.0119 € kWh<sub>el</sub><sup>-1</sup>, respectively (Riley et al., 2020). The lifetime of the CHP unit was  
278 considered to be 20 years (Whiting and Azapagic, 2014). The electricity produced in the  
279 CHP unit was considered to be sold at a price of 0.1283 € kWh<sup>-1</sup> (Eurostat, 2021).

### 280 **2.5 Economic evaluation**

281 The capital expenditures (CAPEX), operating expenditures (OPEX) and electricity  
282 revenue were calculated for the different draw solutes and FO membranes. Eq. (5) and  
283 Eq. (6) were used to calculate the present value (PV) of the gross cost and electricity  
284 revenue, respectively. Subsequently, the PV of the net cost was calculated as the  
285 difference between the PV of the gross cost and the PV of the electricity revenue (Eq.  
286 (7)).

$$287 \quad PV_{GC} = CAPEX + \sum_{t=1}^T \frac{OPEX_t}{(1+i)^t} \quad \text{Eq. (5)}$$

$$288 \quad PV_{ER} = \sum_{t=1}^T \frac{ER_t}{(1+i)^t} \quad \text{Eq. (6)}$$

$$289 \quad PV_{NC} = CAPEX + \sum_{t=1}^T \frac{OPEX_t - ER_t}{(1+i)^t} \quad \text{Eq. (7)}$$

290 where  $PV_{GC}$  is the PV of the gross cost (€),  $PV_{ER}$  is the PV of the electricity revenue (€),  
291  $PV_{NC}$  is the PV of the net cost (€), CAPEX is the capital expenditure (€),  $OPEX_t$  is the  
292 operating expenditure at year  $t$  (€),  $ER_t$  is the electricity revenue at year  $t$  (€),  $i$  is the  
293 discount rate (5%) and  $T$  is the plant lifetime (20 years).

### 294 **3. Results and discussion**

#### 295 **3.1 Impact of draw solute and membrane material on the economic balance of the** 296 **FO+AnMBR system**

297 Figure 2 illustrates the PV of the gross cost, electricity revenue and net cost for the  
298 different draw solutes and both membrane materials. The results show that the net cost of  
299 TFC membrane was substantially lower than the net cost of the CTA membrane  
300 regardless of the draw solute. The difference between both membranes can be mainly  
301 attributed to the higher water permeability and higher solute selectivity of TFC membrane  
302 in comparison with CTA membrane (Table 1). From these results, it is possible to  
303 conclude that the enhanced permselectivity ( $A/B$  ratio) (Shaffer et al., 2015) achieved  
304 with TFC membrane is an important factor influencing the economics of the process. The  
305 structural parameter ( $S$ ), which relates to the properties of the membrane support layer,  
306 was lower for TFC membrane than for CTA membrane (Table 1). In this study, the  
307 membrane properties of the TFC membrane were obtained from Sanahuja-Embuena et  
308 al. (2019), who used a commercial Aquaporin membrane module and reported  $S$  values  
309 lower than commercial CTA membranes. Achieving a low  $S$  parameter is important to  
310 decrease the effect of ICP on the support layer and to increase the effective osmotic  
311 pressure difference between the draw and feed solutions (Blandin et al., 2015). These  
312 results illustrate that the improved properties of novel TFC membranes allowed  
313 increasing the water flux and reducing the draw solute flow rate through the FO

314 membranes, which had a direct impact on FO installation and draw solution  
315 replenishment costs. However, further research is necessary to better understand the  
316 impact of membrane material on the economic balance of the FO+AnMBR system by  
317 using other commercial CTA and TFC membranes.

318 The draw solute had a moderate impact on the economic balance of the FO+AnMBR  
319 system (Figure 2). Regarding CTA membrane, CH<sub>3</sub>COONa and CaCl<sub>2</sub> were the most  
320 economically competitive draw solutes. CH<sub>3</sub>COONa featured a slightly lower net cost  
321 than CaCl<sub>2</sub> despite the higher gross cost of CH<sub>3</sub>COONa. This can be attributed to the  
322 higher electricity revenue achieved in the AnMBR when using CH<sub>3</sub>COONa as draw  
323 solute since the fraction of CH<sub>3</sub>COONa that permeates from the draw solution to the  
324 sewage through the FO membrane is converted into methane. The net cost of MgCl<sub>2</sub> and  
325 Na<sub>2</sub>SO<sub>4</sub> were slightly higher than CH<sub>3</sub>COONa and CaCl<sub>2</sub>. Despite its relatively low FO  
326 membrane fluxes (~4.6 L m<sup>-2</sup> h<sup>-1</sup> LMH), Na<sub>2</sub>SO<sub>4</sub> was one of the most economically  
327 favourable draw solutes (Table 1). The good economic prospect of Na<sub>2</sub>SO<sub>4</sub> can be  
328 attributed to the relatively low RSF of Na<sub>2</sub>SO<sub>4</sub> through FO membranes (~2.5 g m<sup>-2</sup> h<sup>-1</sup>)  
329 that decreased the replenishment costs of the draw solute. However, the presence of  
330 sulphate in the pre-concentrated sewage decreases the amount of energy recovered in the  
331 AnMBR because of the competition between methanogens and sulphate reducing bacteria  
332 (SRB) for the available organic matter (Figure 2). Additionally, the higher concentration  
333 of sulphate in sewage increases the production of H<sub>2</sub>S in the AnMBR that could (i)  
334 partially inhibit anaerobic microorganisms, (ii) increase the requirements for biogas  
335 desulphurisation and (iii) reduce the durability of the infrastructure and hinder the long-  
336 term operability of the AnMBR (out of the scope of the present study).

337 Figure 2 also shows that the economic balance of NaCl, Ca(NO<sub>3</sub>)<sub>2</sub> and KCl was little  
338 attractive since these solutes featured the highest RSF (>4 g m<sup>-2</sup> h<sup>-1</sup>) despite achieving  
339 relatively high FO membrane fluxes (>5.7 L m<sup>-2</sup> h<sup>-1</sup>). This is particularly important for  
340 Ca(NO<sub>3</sub>)<sub>2</sub> because high RSF increases the concentration of nitrate in the sewage that, in  
341 turn, decreases the amount of organic matter available for methane production (Figure 2).  
342 Furthermore, high RSFs could enhance biofouling and scaling on FO active layer due the  
343 interaction of the sewage compounds with the draw solute cations (i.e. Na<sup>+</sup>, Ca<sup>2+</sup>, Mg<sup>2+</sup>)  
344 (She et al., 2012; Zou et al., 2019). These results illustrate that the selection of a suitable  
345 draw solute for FO+AnMBR system requires a compromise solution considering the  
346 capability of the draw solute to achieve high water fluxes with limited RSF.

347 Regarding TFC membrane, MgCl<sub>2</sub> was the most economically favourable draw solute  
348 followed by NaCl and MgSO<sub>4</sub> (Figure 2). This is in agreement with the net cost results  
349 obtained with CTA membrane since the same trend was observed for these three solutes.  
350 However, further experimental work is needed to expand the results of the TFC  
351 membrane by testing other draw solutes, such as KCl, CaCl<sub>2</sub>, Na<sub>2</sub>SO<sub>4</sub>, Ca(NO<sub>3</sub>)<sub>2</sub> and  
352 CH<sub>3</sub>COONa. Finally, it is worth mentioning that MgSO<sub>4</sub> was not economically  
353 favourable for none of the membranes since this draw solute (i) featured a noticeably  
354 lower FO membrane flux in comparison to the other draw solutes and (ii) produced a  
355 limited amount of methane in the AnMBR due to the presence of sulphate in the pre-  
356 concentrated sewage.

### 357 **3.2 Gross cost distribution**

358 Figure 3 shows the gross cost distribution for the different draw solutes and both  
359 membranes. Regarding CTA membrane, the capital cost of the FO system represented the  
360 highest cost contributor (33-39%) for MgCl<sub>2</sub>, CaCl<sub>2</sub>, Na<sub>2</sub>SO<sub>4</sub>, MgSO<sub>4</sub> and CH<sub>3</sub>COONa

361 (Figure 3B). The replacement of the FO membranes during the plant lifetime represented  
362 the second highest impact for these five draw solutes (31-37%). This shows that the costs  
363 associated with the FO installation had a high impact on the net cost for MgCl<sub>2</sub>, CaCl<sub>2</sub>,  
364 Na<sub>2</sub>SO<sub>4</sub>, MgSO<sub>4</sub> and CH<sub>3</sub>COONa. Similar results were obtained for the TFC membrane  
365 since the FO capital cost (33-39%) and FO membrane replacement cost (31-36%)  
366 represented the two highest cost contributors for MgCl<sub>2</sub> and MgSO<sub>4</sub> (Figure 3B).  
367 However, in absolute values, the gross cost contribution of the costs related to FO  
368 installation (i.e. FO capital cost, FO membrane replacement cost, FO draw solution  
369 replenishment cost, maintenance cost and labour cost) were noticeably reduced when  
370 using the TFC membrane because of the better flux performance than CTA membrane  
371 (Figure 3A). These results highlight the importance of achieving high water  
372 permeabilities for the FO+AnMBR system.

373 The FO draw solution replenishment cost represented the highest cost contributor for  
374 CTA membrane using NaCl, KCl and Ca(NO<sub>3</sub>)<sub>2</sub> (29-39%) as draw solutes (Figure 3B).  
375 The high impact of FO draw solution replenishment on the net cost for these three draw  
376 solutes can be attributed to: (i) the high RSF (>4 g m<sup>-2</sup> h<sup>-1</sup>), which increased the necessity  
377 to replenish the solute to keep the draw solute osmotic pressure constant and (ii) the higher  
378 water flux (>5.7 L m<sup>-2</sup> h<sup>-1</sup>) of these solutes, which minimised the contribution of FO  
379 installation to the net cost. The draw solution replenishment cost also represented the  
380 highest cost contributor for TFC membrane when using NaCl (32%) as draw solute  
381 (Figure 3B). However, in absolute values, the gross cost contributor of draw solution  
382 replenishment was also reduced with the TFC membrane because TFC membrane  
383 featured a lower RSF and a higher permselectivity than CTA membrane (Figure 3A). For

384 all draw solutes, the CHP capital and operating costs did not have a high impact on the  
385 net cost since their contribution was below 5% of the gross cost contribution.

### 386 **3.3 Sensitivity analysis**

387 Figure 4 illustrates the net cost of the different draw solutes and membranes for a  $\pm 30\%$   
388 variation of the most relevant economic parameters. The results show that the FO  
389 membrane cost variation had the highest impact on the net cost for all the draw solutes  
390 except for KCl (CTA membrane) and NaCl (TFC membrane). The variation of FO  
391 membrane cost affects both the initial investment and the cost to replace the FO  
392 membranes during the plant lifetime. These results highlight that FO membrane flux is a  
393 key economic driver in the FO+AnMBR system since this determines the FO membrane  
394 area required, which is directly correlated with the FO membrane purchasing and  
395 replacement cost. The variation of the FO membranes lifetime also had a high effect on  
396 the economic balance. This points out the importance to extend the lifetime of FO  
397 membranes to further improve the competitiveness of the system, which could be  
398 achieved by optimising the FO operational conditions and chemical cleaning strategy (Im  
399 et al., 2020). The chemical cost variation had the highest impact on the net cost for KCl  
400 and NaCl in CTA and TFC membranes, respectively (Figure 4). This can be directly  
401 attributed to the high RSF of these draw solutes for CTA and TFC membranes.

402 Figure 4 results also show that the electricity price variation led to small and moderate  
403 changes in the net cost for CTA and TFC membranes, respectively. For CTA, the impact  
404 of electricity price variation on net cost was nearly negligible for  $\text{Na}_2\text{SO}_4$ ,  $\text{MgSO}_4$  and  
405  $\text{Ca}(\text{NO}_3)_2$  since these solutes substantially decreased the production of methane in the  
406 AnMBR and made the electricity revenue irrelevant in comparison to the other cost  
407 contributors. Conversely, the impact of the electricity price variation on the net cost was

408 relatively high when using  $\text{CH}_3\text{COONa}$  as a draw solute since this solute increased the  
409 methane production in the AnMBR. The electricity price variation had a higher impact  
410 on the TFC economic balance since (i) the methane production is similar regardless of  
411 the type of FO membrane used and (ii) the FO-related costs are lower for TFC than for  
412 CTA membranes. These results imply that the superior performance of the TFC  
413 membranes makes the relative importance of electricity revenue higher for TFC  
414 membranes than for CTA membranes.

### 415 **3.4 Impact of draw solute on permeate quality and AnMBR performance**

416 Table 2 shows the COD concentration (both influent and permeate), draw solute  
417 concentration and methane production of the AnMBR for the different draw solutes,  
418 membrane materials and FO recoveries. Besides the 80% FO recovery used in the  
419 previous sections, this section included two additional FO recoveries (i.e. 50 and 90%) to  
420 better understand the impact of sewage pre-concentration on the AnMBR performance  
421 (i.e. methane production and permeate quality).

422 Table 2 results show that the AnMBR COD removal efficiency was similar regardless of  
423 the draw solute and FO membrane material since the permeate COD concentration  
424 remained rather constant at a specific FO recovery condition. These results indicate that,  
425 despite the sewage pre-concentration and RSF, inhibition of the anaerobic biomass would  
426 have a minor impact on AnMBR performance (Table 2). Besides the great adaptability of  
427 anaerobic biomass to operate under harsh conditions, the slight loss of activity due to  
428 inhibition could be mitigated by increasing the concentration of active biomass in the  
429 AnMBR (Chen et al., 2008). The loss of activity could also be mitigated by the capability  
430 of the AnMBR to retain specific microorganisms able to tolerate higher inhibitory

431 concentrations regardless of their doubling time and aggregation properties (Dereli et al.,  
432 2012; Puyol et al., 2017).

433 Methane production was similar for NaCl, MgCl<sub>2</sub>, KCl and CaCl<sub>2</sub> regardless of the FO  
434 membrane material and FO recovery (Table 2). However, methane production  
435 substantially decreased when using Na<sub>2</sub>SO<sub>4</sub>, MgSO<sub>4</sub> and Ca(NO<sub>3</sub>)<sub>2</sub> as draw solutes since  
436 these solutes decreased the amount of organic matter available for methanisation. For  
437 these draw solutes, the amount of methane produced progressively decreased as the FO  
438 recovery increased due to the higher concentration of draw solute in the pre-concentrated  
439 sewage at higher FO recoveries. This was particularly noticeable for Ca(NO<sub>3</sub>)<sub>2</sub> since the  
440 RSF of Ca(NO<sub>3</sub>)<sub>2</sub> was substantially higher than MgSO<sub>4</sub> and Na<sub>2</sub>SO<sub>4</sub>. Accordingly, the  
441 high presence of nitrate in the pre-concentrated sewage sharply decreased methane  
442 production at FO recoveries of 80 and 90%. CH<sub>3</sub>COONa achieved the highest methane  
443 production among the different draw solutes because this draw solute increased the  
444 amount of easily biodegradable organic matter in the pre-concentrated sewage, which  
445 allowed maximising methane production in the AnMBR.

446 Increasing the pre-concentration factor has a direct impact on AnMBR permeate quality.  
447 The permeate COD concentration increased as the FO recovery increased, increasing both  
448 the concentration of biodegradable organic matter (S<sub>S</sub>) and the concentration of soluble  
449 inerts (S<sub>I</sub>). This phenomenon was particularly important for the high FO recovery  
450 scenarios (80 and 90%) since the permeate COD concentration could exceed the  
451 European Union COD discharge limits (<125 mg COD L<sup>-1</sup>) (CEC, 1991). Additionally,  
452 the nitrogen and phosphorus concentrations in the permeate also increase with the FO  
453 recovery. For this reason, the implementation of post-treatments would be necessary to

454 meet the effluent discharge limits for COD and nutrients when FO and AnMBR  
455 technologies are combined.

456 The draw solute concentration also increased with the FO recovery. For the CTA  
457 membrane, the NaCl concentration increased from 0.65 to 5.89 mg L<sup>-1</sup> as the FO recovery  
458 increased from 50 to 90% (Table 2). However, the NaCl concentration in the pre-  
459 concentrated sewage was substantially decreased using TFC membrane due to its higher  
460 permselectivity. Compared to the CTA membrane, TFC membrane decreased the NaCl,  
461 MgCl<sub>2</sub> and MgSO<sub>4</sub> concentrations in the pre-concentrated sewage by 3, 8 and 11 times,  
462 respectively (Table 2). These results indicate that high FO recoveries could result in a  
463 permeate and digestate with a high salinity concentration, which could limit their  
464 application in agriculture as irrigation water and fertilizers (Vinardell et al., 2021). The  
465 production of digestates with high salinities would make necessary to apply other  
466 management alternatives such as incineration or landfilling. Accordingly, restricting the  
467 FO recovery could be used as a strategy to (i) meet the effluent discharge requirements  
468 and (ii) improve the quality of the permeate and digestate to make it suitable for  
469 agricultural application. These two factors are paramount to make the FO+AnMBR  
470 approach environmentally and technically feasibility.

#### 471 **4. Conclusions**

472 The techno-economic analysis of the FO+AnMBR system showed that FO membrane  
473 material was a determinant economic factor since the net cost of the TFC membrane was  
474 substantially lower than the CTA membrane. The draw solute had a moderate impact on  
475 the FO+AnMBR system economic balance. The capital cost of the FO system was the  
476 most important cost contributor for MgCl<sub>2</sub>, CaCl<sub>2</sub>, Na<sub>2</sub>SO<sub>4</sub>, MgSO<sub>4</sub> and CH<sub>3</sub>COONa (33-

477 39%), whereas ~~while~~ the FO draw solution replenishment was the most important cost  
478 contributor for NaCl, KCl and Ca(NO<sub>3</sub>)<sub>2</sub> (29-32%). The most economically favourable  
479 draw solutes were CH<sub>3</sub>COONa and CaCl<sub>2</sub> for the CTA membrane and MgCl<sub>2</sub> for the TFC  
480 membrane due to their capacity to achieve relatively high water fluxes with low RSF. The  
481 AnMBR COD removal efficiency (>90%) was similar regardless of the draw solute and  
482 membrane material. However, FO recoveries above 80% could compromise the  
483 fulfilment of the permeate discharge requirements. Future experimental research using  
484 different commercial CTA/TFC FO membranes and draw solutes is needed to expand and  
485 complement the results obtained in the present study. Overall, the results from this techno-  
486 economic study highlight that selecting FO membranes and draw solutes capable to  
487 achieve high water fluxes with reduced RSF is crucial to boost the economic  
488 competitiveness of the system and fulfil the permeate discharge requirements.

#### 489 **Acknowledgments**

490 This work was supported by the European Union LIFE programme (LIFE Green Sewer  
491 project, LIFE17 ENV/ES/000341). The authors also acknowledge the grant overseen by  
492 the French National Research Agency (ANR) as part of the “JCJC” Program BâMAN  
493 (ANR-18-CE04-0001-01). Sergi Vinardell is grateful to the Generalitat de Catalunya for  
494 his predoctoral FI grant (2019 FI\_B 00394). Sergi Astals is grateful to the Spanish  
495 Ministry of Science, Innovation and Universities for his Ramon y Cajal fellowship (RYC-  
496 2017-22372). Gaetan Blandin received the support of a fellowship from ”la Caixa”  
497 Foundation (ID 100010434). The fellowship code is LCF/BQ/PR21/11840009. Finally,  
498 the authors would like to thank the Catalan Government for the quality accreditation given  
499 to Environmental Biotechnology research group (2017 SGR 1218).

500 **Declaration of competing interests**

501 The authors declare that they have no known competing financial interests or personal  
502 relationships that could have appeared to influence the work reported in this paper. The  
503 authors also declare that this manuscript reflects only the authors' view and that the  
504 Executive Agency for SME/EU Commission are not responsible for any use that may be  
505 made of the information it contains.

506 **References**

507 Achilli, A., Cath, T.Y., Childress, A.E., 2010. Selection of inorganic-based draw  
508 solutions for forward osmosis applications. *J. Memb. Sci.* 364, 233–241.

509 Almoalimi, K., Liu, Y.-Q., 2022. Enhancing ammonium rejection in forward osmosis for  
510 wastewater treatment by minimizing cation exchange. *J. Memb. Sci.* 648, 120365.

511 Anjum, F., Khan, I.M., Kim, J., Aslam, M., Blandin, G., Heran, M., Lesage, G., 2021.  
512 Trends and progress in AnMBR for domestic wastewater treatment and their impacts  
513 on process efficiency and membrane fouling. *Environ. Technol. Innov.* 21, 101204.

514 Ansari, A.J., Hai, F.I., Guo, W., Ngo, H.H., Price, W.E., Nghiem, L.D., 2015. Selection  
515 of forward osmosis draw solutes for subsequent integration with anaerobic treatment  
516 to facilitate resource recovery from wastewater. *Bioresour. Technol.* 191, 30–36.

517 Ansari, A.J., Hai, F.I., Price, W.E., Drewes, J.E., Nghiem, L.D., 2017. Forward osmosis  
518 as a platform for resource recovery from municipal wastewater - A critical  
519 assessment of the literature. *J. Memb. Sci.* 529, 195–206.

520 Ansari, A.J., Hai, F.I., Price, W.E., Ngo, H.H., Guo, W., Nghiem, L.D., 2018. Assessing  
521 the integration of forward osmosis and anaerobic digestion for simultaneous

522 wastewater treatment and resource recovery. *Bioresour. Technol.* 260, 221–226.

523 Arcanjo, G.S., Costa, F.C.R., Ricci, B.C., Mounteer, A.H., de Melo, E.N.M.L.,  
524 Cavalcante, B.F., Araújo, A. V., Faria, C. V., Amaral, M.C.S., 2020. Draw solution  
525 solute selection for a hybrid forward osmosis-membrane distillation module: Effects  
526 on trace organic compound rejection, water flux and polarization. *Chem. Eng. J.* 400,  
527 125857.

528 Ariesyady, H.D., Ito, T., Okabe, S., 2007. Functional bacterial and archaeal community  
529 structures of major trophic groups in a full-scale anaerobic sludge digester. *Water*  
530 *Res.* 41, 1554–1568.

531 Awad, A.M., Jalab, R., Minier-Matar, J., Adham, S., Nasser, M.S., Judd, S.J., 2019. The  
532 status of forward osmosis technology implementation. *Desalination* 461, 10–21.

533 Bacaksiz, A.M., Kaya, Y., Aydiner, C., 2021. Techno-economic preferability of cost-  
534 performance effective draw solutions for forward osmosis and osmotic anaerobic  
535 bioreactor applications. *Chem. Eng. J.* 410, 127535.

536 Blandin, G., Galizia, A., Monclús, H., Lesage, G., Héran, M., Martinez-Lladó, X., 2021.  
537 Submerged osmotic processes: Design and operation of hollow fiber forward  
538 osmosis modules. *Desalination* 518, 115281.

539 Blandin, G., Verliefe, A.R.D., Tang, C.Y., Le-Clech, P., 2015. Opportunities to reach  
540 economic sustainability in forward osmosis–reverse osmosis hybrids for seawater  
541 desalination. *Desalination* 363, 26–36.

542 Cabrera-Castillo, E.H., Castillo, I., Ciudad, G., Jeison, D., Ortega-Bravo, J.C., 2021. FO-  
543 MD setup analysis for acid mine drainage treatment in Chile: An experimental-

544 theoretical economic assessment compared with FO-RO and single RO.  
545 Desalination 514, 115164.

546 CEC, 1991. Council Directive of 21 May 1991 concerning waste water treatment  
547 (91/271/EEC). Off. J. Eur. Communities No. L 135/40-52.

548 Chen, Y., Cheng, J.J., Creamer, K.S., 2008. Inhibition of anaerobic digestion process: A  
549 review. *Bioresour. Technol.* 99, 4044-4064.

550 Coday, B.D., Heil, D.M., Xu, P., Cath, T.Y., 2013. Effects of transmembrane hydraulic  
551 pressure on performance of forward osmosis membranes. *Environ. Sci. Technol.* 47,  
552 2386–2393.

553 Dereli, R.K., Ersahin, M.E., Ozgun, H., Ozturk, I., Jeison, D., van der Zee, F., van Lier,  
554 J.B., 2012. Potentials of anaerobic membrane bioreactors to overcome treatment  
555 limitations induced by industrial wastewaters. *Bioresour. Technol.* 122, 160–170.

556 Eurostat, 2021. Electricity price statistics. [https://ec.europa.eu/eurostat/statistics-  
557 explained/index.php?title=Electricity\\_price\\_statistics#Electricity\\_prices\\_for\\_non-  
558 household\\_consumers](https://ec.europa.eu/eurostat/statistics-explained/index.php?title=Electricity_price_statistics#Electricity_prices_for_non-household_consumers). (accessed 8 March, 2022).

559 Ferby, M., Zou, S., He, Z., 2020. Reduction of reverse solute flux induced solute buildup  
560 in the feed solution of forward osmosis. *Environ. Sci. Water Res. Technol.* 6, 423–  
561 435.

562 Ferrari, F., Balcazar, J.L., Rodriguez-Roda, I., Pijuan, M., 2019. Anaerobic membrane  
563 bioreactor for biogas production from concentrated sewage produced during sewer  
564 mining. *Sci. Total Environ.* 670, 993–1000.

565 Fritzmann, C., Löwenberg, J., Wintgens, T., Melin, T., 2007. State-of-the-art reverse

566 osmosis desalination. *Desalination* 216, 1–76.

567 Hu, Y., Du, R., Nitta, S., Ji, J., Rong, C., Cai, X., Qin, Y., Li, Y.Y., 2021. Identification  
568 of sustainable filtration mode of an anaerobic membrane bioreactor for wastewater  
569 treatment towards low-fouling operation and efficient bioenergy production. *J.*  
570 *Clean. Prod.* 329.

571 Im, S.J., Jeong, Sanghyun, Jeong, Seongpil, Jang, A., 2020. Techno-economic evaluation  
572 of an element-scale forward osmosis-reverse osmosis hybrid process for seawater  
573 desalination. *Desalination* 476, 114240.

574 Irvine, G.J., Rajesh, S., Georgiadis, M., Phillip, W.A., 2013. Ion selective permeation  
575 through cellulose acetate membranes in forward osmosis. *Environ. Sci. Technol.* 47,  
576 13745–13753.

577 Kim, J.E., Phuntsho, S., Chekli, L., Hong, S., Ghaffour, N., Leiknes, T.O., Choi, J.Y.,  
578 Shon, H.K., 2017. Environmental and economic impacts of fertilizer drawn forward  
579 osmosis and nanofiltration hybrid system. *Desalination* 416, 76–85.

580 Kim, M. kyu, Chang, J.W., Park, K., Yang, D.R., 2022. Comprehensive assessment of  
581 the effects of operating conditions on membrane intrinsic parameters of forward  
582 osmosis (FO) based on principal component analysis (PCA). *J. Memb. Sci.* 641,  
583 119909.

584 Krzeminski, P., Leverette, L., Malamis, S., Katsou, E., 2017. Membrane bioreactors – A  
585 review on recent developments in energy reduction, fouling control, novel  
586 configurations, LCA and market prospects. *J. Memb. Sci.* 527, 207–227.

587 Lutchmiah, K., Verliefde, A.R.D., Roest, K., Rietveld, L.C., Cornelissen, E.R., 2014.

588 Forward osmosis for application in wastewater treatment: A review. *Water Res.* 58,  
589 179-197.

590 Maaz, M., Yasin, M., Aslam, M., Kumar, G., Atabani, A.E., Idrees, M., Anjum, F., Jamil,  
591 F., Ahmad, R., Khan, A.L., Lesage, G., Heran, M., Kim, J., 2019. Anaerobic  
592 membrane bioreactors for wastewater treatment: Novel configurations, fouling  
593 control and energy considerations. *Bioresour. Technol.* 283, 358–372.

594 Metcalf & Eddy, 2014. *Wastewater Engineering: Treatment and Resource Recovery*.  
595 Fifth ed. McGraw Hill, New York.

596 Puyol, D., Batstone, D.J., Hülsen, T., Astals, S., Peces, M., Krömer, J.O., 2017. Resource  
597 recovery from wastewater by biological technologies: Opportunities, challenges,  
598 and prospects. *Front. Microbiol.* 7.

599 Riley, D.M., Tian, J., Güngör-Demirci, G., Phelan, P., Rene Villalobos, J., Milcarek, R.J.,  
600 2020. Techno-economic assessment of CHP systems in wastewater treatment plants.  
601 *Environments* 7, 1–32.

602 Sanahuja-Embuena, V., Khensir, G., Yusuf, M., Andersen, M.F., Nguyen, X.T.,  
603 Trzaskus, K., Pinelo, M., Helix-Nielsen, C., 2019. Role of operating conditions in a  
604 pilot scale investigation of hollow fiber forward osmosis membrane modules.  
605 *Membranes.* 9, 66.

606 Shaffer, D.L., Werber, J.R., Jaramillo, H., Lin, S., Elimelech, M., 2015. Forward osmosis:  
607 Where are we now? *Desalination* 356, 271–284.  
608 <https://doi.org/10.1016/j.desal.2014.10.031>

609 She, Q., Jin, X., Li, Q., Tang, C.Y., 2012. Relating reverse and forward solute diffusion

610 to membrane fouling in osmotically driven membrane processes. *Water Res.* 46,  
611 2478–2486.

612 Tiraferri, A., Yip, N.Y., Straub, A.P., Romero-Vargas Castrillon, S., Elimelech, M., 2013.  
613 A method for the simultaneous determination of transport and structural parameters  
614 of forward osmosis membranes. *J. Memb. Sci.* 444, 523–538.

615 Valladares Linares, R., Li, Z., Yangali-Quintanilla, V., Ghaffour, N., Amy, G., Leiknes,  
616 T., Vrouwenvelder, J.S., 2016. Life cycle cost of a hybrid forward osmosis – low  
617 pressure reverse osmosis system for seawater desalination and wastewater recovery.  
618 *Water Res.* 88, 225–234.

619 Vinardell, S., Astals, S., Jaramillo, M., Mata-Alvarez, J., Dosta, J., 2021. Anaerobic  
620 membrane bioreactor performance at different wastewater pre-concentration factors:  
621 An experimental and economic study. *Sci. Total Environ.* 750, 141625.

622 Vinardell, S., Astals, S., Mata-Alvarez, J., Dosta, J., 2020a. Techno-economic analysis of  
623 combining forward osmosis-reverse osmosis and anaerobic membrane bioreactor  
624 technologies for municipal wastewater treatment and water production. *Bioresour.*  
625 *Technol.* 297, 122395.

626 Vinardell, S., Astals, S., Peces, M., Cardete, M.A., Fernández, I., Mata-Alvarez, J., Dosta,  
627 J., 2020b. Advances in anaerobic membrane bioreactor technology for municipal  
628 wastewater treatment: A 2020 updated review. *Renew. Sustain. Energy Rev.* 130,  
629 109936.

630 Wang, J., Liu, X., 2021. Forward osmosis technology for water treatment: Recent  
631 advances and future perspectives. *J. Clean. Prod.* 280, 124354.

632 Whiting, A., Azapagic, A., 2014. Life cycle environmental impacts of generating  
633 electricity and heat from biogas produced by anaerobic digestion. *Energy* 70, 181–  
634 193.

635 Yangali-Quintanilla, V., Olesen, L., Lorenzen, J., Rasmussen, C., Laursen, H.,  
636 Vestergaard, E., Keiding, K., 2015. Lowering desalination costs by alternative  
637 desalination and water reuse scenarios. *Desalin. Water Treat.* 55, 2437–2445.

638 Zahedi, S., Ferrari, F., Blandin, G., Balcazar, J.L., Pijuan, M., 2021. Enhancing biogas  
639 production from the anaerobic treatment of municipal wastewater by forward  
640 osmosis pretreatment. *J. Clean. Prod.* 315, 128140.

641 Zhang, X., Liu, Y., 2022. Circular economy is game-changing municipal wastewater  
642 treatment technology towards energy and carbon neutrality. *Chem. Eng. J.* 429,  
643 132114.

644 Zhen, G., Pan, Y., Lu, X., Li, Y.-Y., Zhang, Z., Niu, C., Kumar, G., Kobayashi, T., Zhao,  
645 Y., Xu, K., 2019. Anaerobic membrane bioreactor towards biowaste biorefinery and  
646 chemical energy harvest: Recent progress, membrane fouling and future  
647 perspectives. *Renew. Sustain. Energy Rev.* 115, 109392.

648 Zou, S., Qin, M., He, Z., 2019. Tackle reverse solute flux in forward osmosis towards  
649 sustainable water recovery: reduction and perspectives. *Water Res.* 149, 362–374.

650

**Table 1.** A, B and S parameters as well as main properties and costs for the different draw solutes and membranes under study.

	CTA Membrane								TFC Membrane		
	NaCl	MgCl <sub>2</sub>	KCl	CaCl <sub>2</sub>	Na <sub>2</sub> SO <sub>4</sub>	MgSO <sub>4</sub>	Ca(NO <sub>3</sub> ) <sub>2</sub>	CH <sub>3</sub> COONa	NaCl	MgCl <sub>2</sub>	MgSO <sub>4</sub>
A (L m <sup>-2</sup> h <sup>-1</sup> bar <sup>-1</sup> ) <sup>a</sup>	0.55	0.55	0.55	0.55	0.55	0.55	0.55	0.55	1.71	1.71	1.71
S (mm) <sup>a</sup>	0.463	0.463	0.463	0.463	0.463	0.463	0.463	0.463	0.14	0.14	0.14
B (L m <sup>-2</sup> h <sup>-1</sup> ) <sup>b</sup>	0.303	0.215	0.363	0.268	0.091	0.04	0.15	0.073	0.240	0.07	0.01
D (×10 <sup>-9</sup> m <sup>2</sup> s <sup>-1</sup> ) <sup>c</sup>	1.47	1.05	1.86	1.13	0.76	0.37	1.28	1.44	1.47	1.05	0.37
k (×10 <sup>5</sup> m s <sup>-1</sup> ) <sup>d</sup>	1.99	1.59	2.32	1.67	1.28	0.79	1.81	1.96	1.99	1.59	0.79
Initial osmotic pressure (bar)	28	28	28	28	28	28	28	28	28	28	28
Initial draw solute concentration (g L <sup>-1</sup> ) <sup>e</sup>	35.2	34.2	47.0	43.8	84.7	141.3	87.2	55.9	35.2	34.2	141.3
Cation concentration (g L <sup>-1</sup> )	13.8	8.7	24.7	15.8	27.4	28.5	21.3	15.7	13.8	8.7	28.5
Anion concentration (g L <sup>-1</sup> )	21.4	25.5	22.3	28.0	57.3	112.8	65.9	40.2	21.4	25.5	112.8
Draw solute purchase cost (€ mol <sup>-1</sup> ) <sup>f</sup>	0.016	0.025	0.020	0.015	0.013	0.017	0.038	0.034	0.016	0.025	0.017

<sup>a</sup> Coday et al. (2013) for CTA membrane and Sanahuja-Embuena et al. (2019) for TFC membrane.

<sup>b</sup> Calculated from data provided by Achilli et al. (2010) and Ansari et al. (2015) for CTA membrane and Sanahuja-Embuena et al. (2019) for TFC membrane.

<sup>c</sup> Achilli et al. (2010) for NaCl, MgCl<sub>2</sub>, KCl, CaCl<sub>2</sub>, Na<sub>2</sub>SO<sub>4</sub> and MgSO<sub>4</sub>, Irvine et al. (2013) for Ca(NO<sub>3</sub>)<sub>2</sub> and Ansari et al. (2015) for CH<sub>3</sub>COONa.

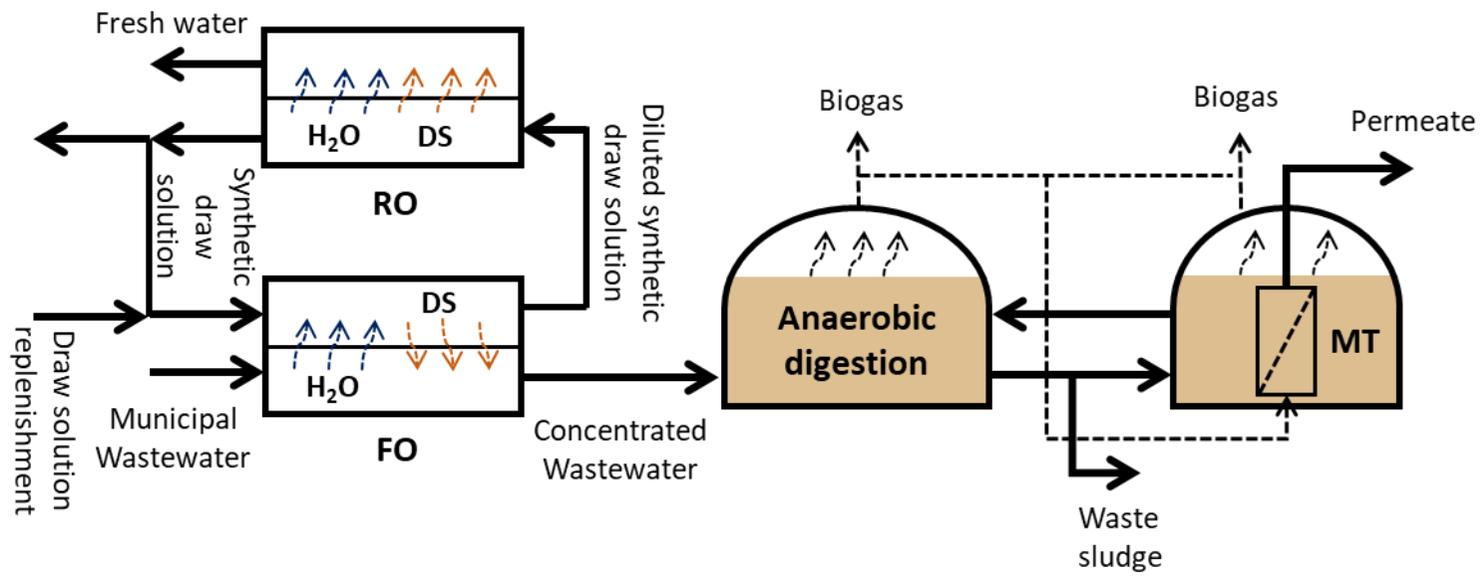
<sup>d</sup> The k parameter was calculated from Sanahuja-Embuena et al. (2019) equations and parameters.

<sup>e</sup> Achilli et al. (2010) for NaCl, MgCl<sub>2</sub>, KCl, CaCl<sub>2</sub>, Na<sub>2</sub>SO<sub>4</sub>, MgSO<sub>4</sub> and Ca(NO<sub>3</sub>)<sub>2</sub> and calculated from data provided by Arcanjo et al. (2020) for CH<sub>3</sub>COONa.

<sup>f</sup> Data obtained from Bacaksiz et al. (2021).

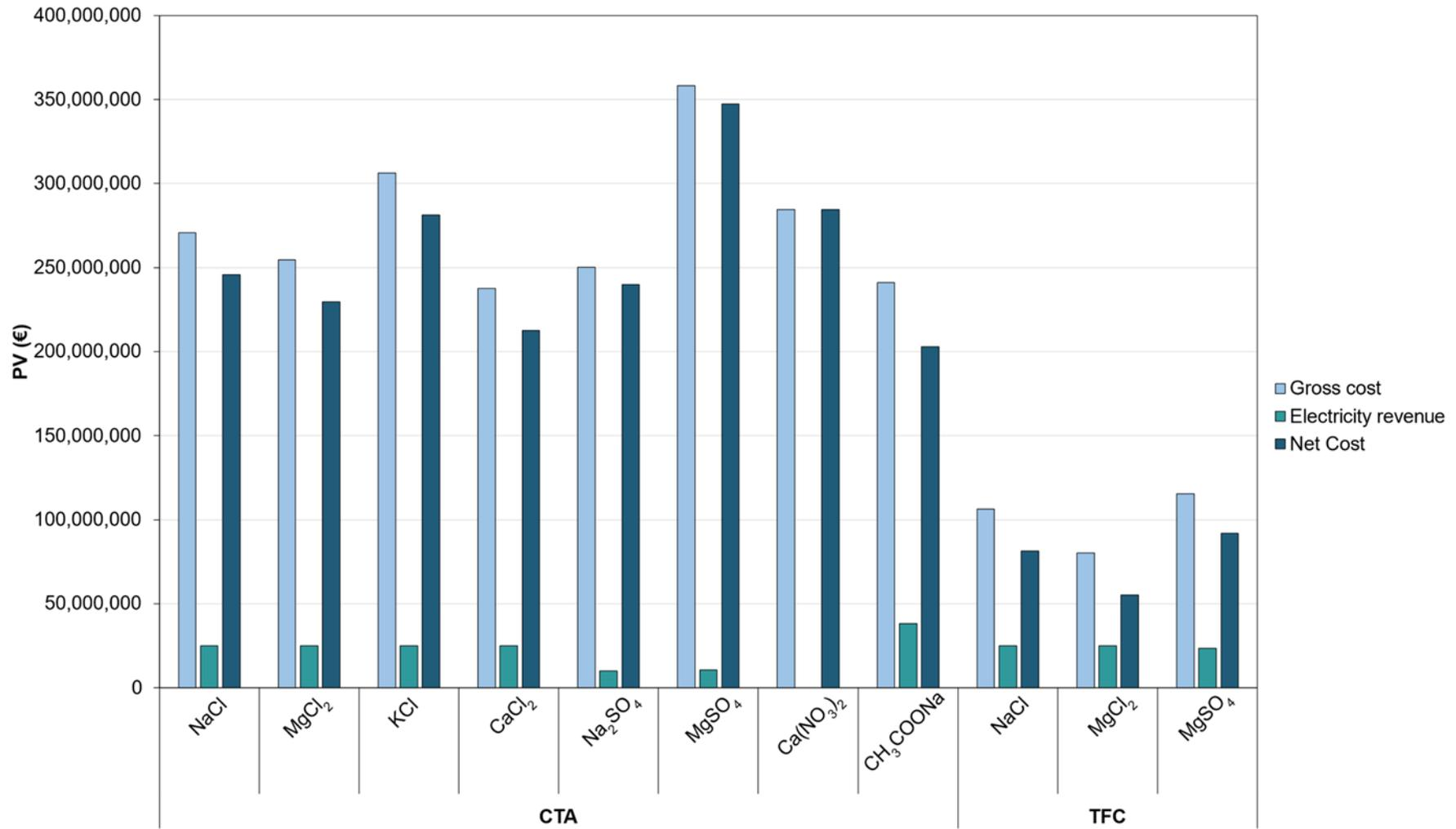
**Table 2.** AnMBR performance and permeate quality for the different draw solutes and membranes under study. The AnMBR performance was modelled for an FO recovery of 50, 80 and 90%.

		CTA Membrane								TFC Membrane		
		NaCl	MgCl <sub>2</sub>	KCl	CaCl <sub>2</sub>	Na <sub>2</sub> SO <sub>4</sub>	MgSO <sub>4</sub>	Ca(NO <sub>3</sub> ) <sub>2</sub>	CH <sub>3</sub> COONa	NaCl	MgCl <sub>2</sub>	MgSO <sub>4</sub>
R=50%	Influent COD concentration (mg L <sup>-1</sup> )	840	840	840	840	840	840	840	929	840	840	840
	Influent solute concentration (g L <sup>-1</sup> )	0.65	0.47	1.02	0.73	0.55	0.45	0.88	0.29	0.19	0.06	0.04
	Permeate COD concentration (mg L <sup>-1</sup> )	83.0	83.7	84.4	83.6	82.7	83.3	83.3	91.1	82.4	82.3	82.2
	Methane production (Nm <sup>3</sup> d <sup>-1</sup> )	10,992	10,991	10,989	10,991	6,621	6,790	3,462	14,927	10,993	10,993	10,617
	Electricity production (kWh d <sup>-1</sup> )	39,968	38,964	39,960	39,964	24,076	24,690	12,589	54,278	39,971	39,997	38,604
R=80%	Influent COD concentration (mg L <sup>-1</sup> )	2,100	2,100	2,100	2,100	2,100	2,100	2,100	2,454	2,100	2,100	2,100
	Influent solute concentration (g L <sup>-1</sup> )	2.61	1.88	4.07	2.93	2.20	1.80	3.53	1.16	0.78	0.23	0.16
	Permeate COD concentration (mg L <sup>-1</sup> )	176.5	179.4	182.7	179.2	175.3	177.7	178.0	189.5	173.9	173.6	173.2
	Methane production (Nm <sup>3</sup> d <sup>-1</sup> )	11,745	11,743	11,742	11,744	4,753	5,023	0	18,053	11,747	11,747	11,145
	Electricity production (kWh d <sup>-1</sup> )	42,708	42,702	42,696	42,703	17,281	18,263	0	65,643	42,713	42,713	40,526
R=90%	Influent COD concentration (mg L <sup>-1</sup> )	4,200	4,200	4,200	4,200	4,200	4,200	4,200	4,998	4,200	4,200	4,200
	Influent solute concentration (g L <sup>-1</sup> )	5.89	4.22	9.16	6.58	4.96	4.04	7.93	2.60	1.75	0.52	0.36
	Permeate COD concentration (mg L <sup>-1</sup> )	331.6	338.8	347.3	338.3	328.9	334.7	335.3	344.8	325.5	324.8	324.0
	Methane production (Nm <sup>3</sup> d <sup>-1</sup> )	11,996	11,994	11,993	11,995	4,130	4,433	0	19,096	11,998	11,998	11,321
	Electricity production (kWh d <sup>-1</sup> )	43,621	43,614	43,608	43,615	15,016	16,121	0	69,438	43,627	43,627	41,166

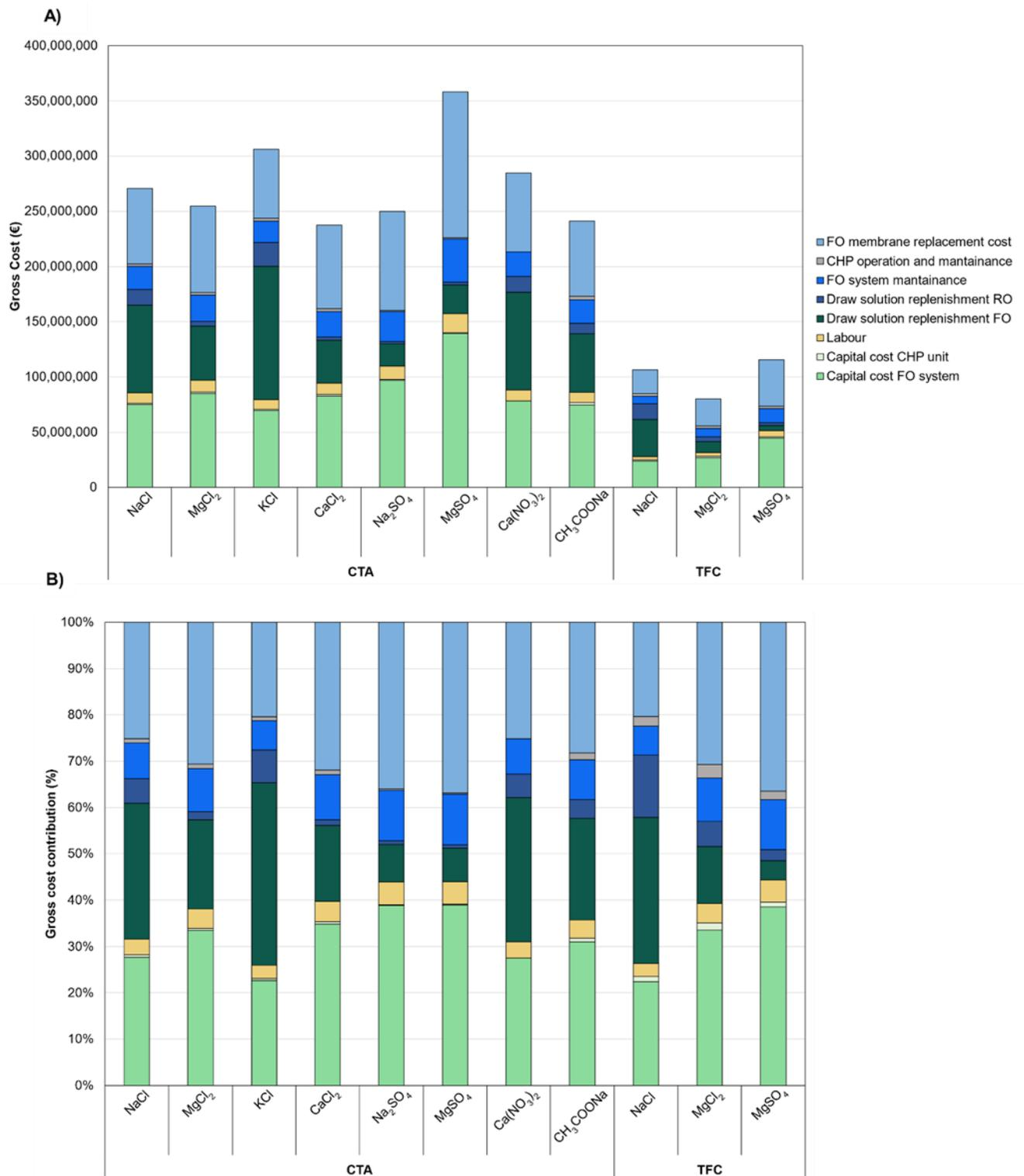


**Figure 1.** Closed-loop configuration integrating FO, RO and AnMBR technologies for municipal sewage treatment and water production (adapted from Vinardell et al.

(2020a)).



**Figure 2.** Present value (PV) of the gross cost, electricity revenue and net cost for the different draw solutes and membranes under study.



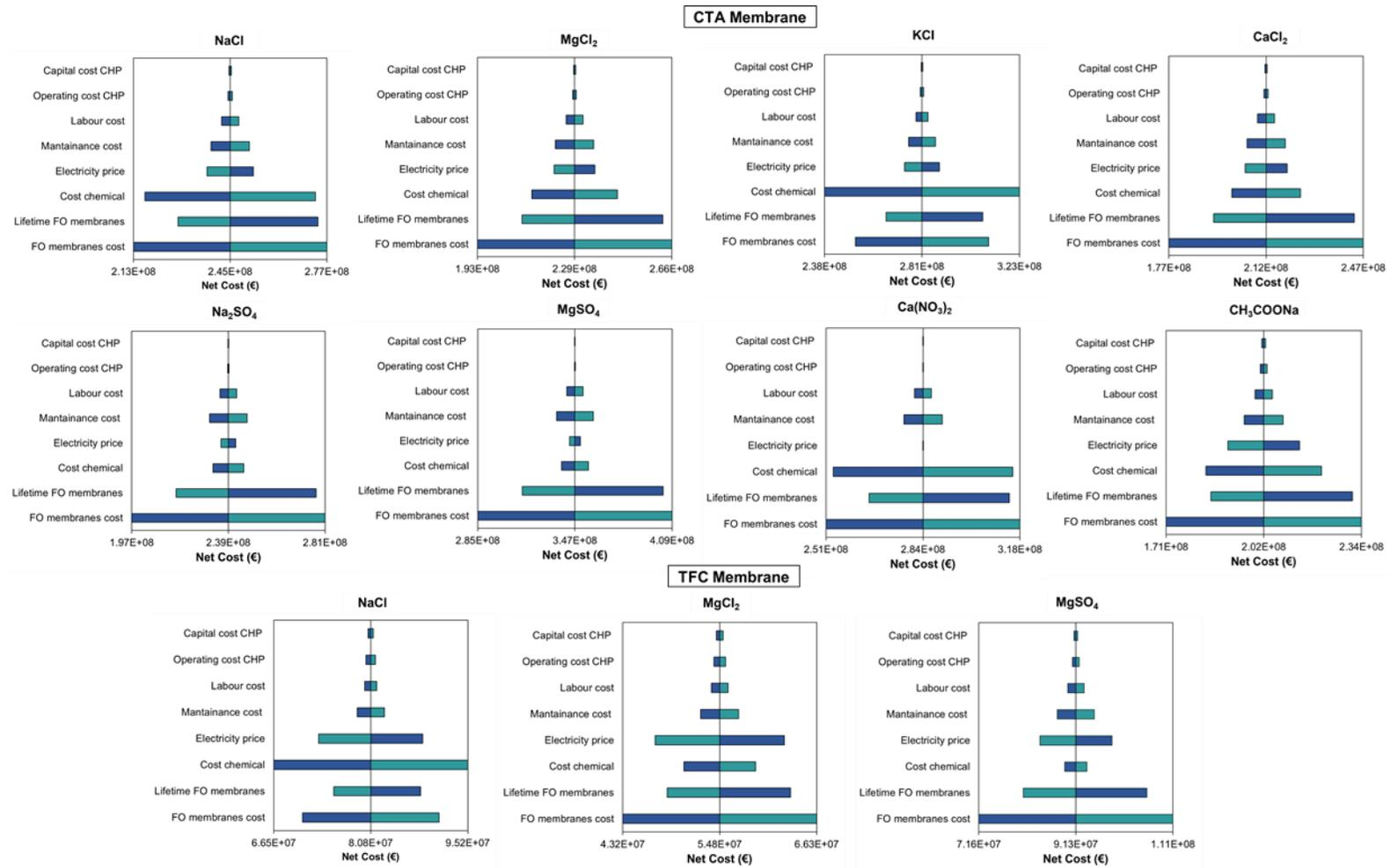


**Figure 4.** Sensitivity analysis of the net cost for a  $\pm 30\%$  variation of the most important economic parameters for the different draw solutes and membranes under study.